

# Glucose Induces Opposite Intracellular $\text{Ca}^{2+}$ Concentration Oscillatory Patterns in Identified $\alpha$ - and $\beta$ -Cells Within Intact Human Islets of Langerhans

Ivan Quesada,<sup>1</sup> Mariana G. Todorova,<sup>1</sup> Paloma Alonso-Magdalena,<sup>1</sup> Marta Beltrá,<sup>1</sup> Everardo M. Carneiro,<sup>4</sup> Franz Martin,<sup>2</sup> Angel Nadal,<sup>1</sup> and Bernat Soria<sup>3</sup>

Homeostasis of blood glucose is mainly regulated by the coordinated secretion of glucagon and insulin from  $\alpha$ - and  $\beta$ -cells within the islets of Langerhans. The release of both hormones is  $\text{Ca}^{2+}$  dependent. In the current study, we used confocal microscopy and immunocytochemistry to unequivocally characterize the glucose-induced  $\text{Ca}^{2+}$  signals in  $\alpha$ - and  $\beta$ -cells within intact human islets. Extracellular glucose stimulation induced an opposite response in these two cell types. Although the intracellular  $\text{Ca}^{2+}$  concentration ( $[\text{Ca}^{2+}]_i$ ) in  $\beta$ -cells remained stable at low glucose concentrations,  $\alpha$ -cells exhibited an oscillatory  $[\text{Ca}^{2+}]_i$  response. Conversely, the elevation of extracellular glucose elicited an oscillatory  $[\text{Ca}^{2+}]_i$  pattern in  $\beta$ -cells but inhibited low-glucose-induced  $[\text{Ca}^{2+}]_i$  signals in  $\alpha$ -cells. These  $\text{Ca}^{2+}$  signals were synchronic among  $\beta$ -cells grouped in clusters within the islet, although they were not coordinated among the whole  $\beta$ -cell population. The response of  $\alpha$ -cells was totally asynchronous. Therefore, both the  $\alpha$ - and  $\beta$ -cell populations within human islets did not work as a syncytium in response to glucose. A deeper knowledge of  $\alpha$ - and  $\beta$ -cell behavior within intact human islets is important to better understand the physiology of the human endocrine pancreas and may be useful to select high-quality islets for transplantation. *Diabetes* 55:2463–2469, 2006

**A**t present, allogeneic transplantation of islets may represent an actual cure for type 1 diabetic patients (1,2). Islet quality before transplantation is essential, and different methods are still being developed to improve it (3). Given the existence of important functional and structural divergences compared

with animal models (4–6), a deeper knowledge of islet physiology in humans is necessary to understand its function and regulation. Moreover, it can help to establish parameters and criteria to select high-quality functional islets for transplantation (3). Glucose homeostasis is mainly regulated by the secretory response of the islet of Langerhans (7–9). The integral function of this endocrine unit depends on the interaction and secretion of different cell types, mainly  $\alpha$ - and  $\beta$ -cells (7–10). When extracellular glucose concentrations become low,  $\alpha$ -cells release the hyperglycemic hormone glucagon, whereas in the presence of high concentrations of sugar,  $\beta$ -cells secrete insulin to restore normal glucose levels (7,11–15). Islet cell function and glucose homeostasis are further regulated by multiple levels of control and the interaction with several organs (7–9). Failures in this system may lead to the widespread disease diabetes (8). The hyperglycemia provoked by diabetes is mainly caused by a malfunction of insulin secretion from  $\beta$ -cells or an adaptation to increased peripheral demand (16), although a disturbed secretion of glucagon from  $\alpha$ -cells may exacerbate it (17,18). Additionally, in insulin-treated diabetic patients, impaired control of glucagon secretion from  $\alpha$ -cells can provoke acute insulin-induced hypoglycemia, a major complication that may cause death (19). Hence, a profound knowledge of the regulation of both  $\beta$ - and  $\alpha$ -cell populations is necessary to understand the complex control of glycemia during physiological and pathological situations.

Although  $\alpha$ -cells play an important role in the control of glycemia, most of the information from islet physiology comes from studies performed in  $\beta$ -cells. The study of  $\alpha$ -cells has been complicated because of the scarcity of this cell population in the islet, a lack of identification patterns, and a lack of resolution of conventional techniques. In the last few years, several groups have characterized the electrophysiological properties and  $\text{Ca}^{2+}$  signals in response to glucose of the main cell types in the intact islet of the mouse (12–15). These studies have shown that the  $\text{Ca}^{2+}$  signals that lead to secretion are a consequence of the characteristic electrical activity of each cell type. In the case of the  $\beta$ -cell, all of these cellular events are stimulated at high glucose concentrations and occur in an oscillatory manner (20–22). On the other hand, electrical activity, intracellular  $\text{Ca}^{2+}$  concentration ( $[\text{Ca}^{2+}]_i$ ) signals, and, consequently, glucagon release from  $\alpha$ -cells is stimulated at low glucose levels (11–15). In hypoglycemic conditions,  $[\text{Ca}^{2+}]_i$  oscillates in the  $\alpha$ -cell. When the extracellular glucose concentration increases to

From the <sup>1</sup>Institute of Bioengineering, Miguel Hernandez University, Sant Joan d'Alacant, Spain; the <sup>2</sup>Andalusian Center of Developmental Biology, University Pablo Olavide, Seville, Spain; <sup>3</sup>CABIMER (Andalusian Center for Molecular Biology and Regenerative Medicine), Seville, Spain; and the <sup>4</sup>Department of Physiology and Biology, State University of Campinas, Campinas, Brazil.

Address correspondence and reprint requests to Ivan Quesada, PhD, Institute of Bioengineering, Miguel Hernandez University, Ctra. N-332, Km. 87, 03550 Sant Joan d'Alacant, Spain. E-mail: ivanq@umh.es.

Correspondence and reprint requests may also be addressed to Bernat Soria, MD, PhD, CABIMER, Andalusian Center for Molecular Biology and Regenerative Medicine, Avda. Américo Vespucio s/n, Isla de la Cartuja, 41092 Seville, Spain. E-mail: bernat.soria@juntadeandalucia.es.

Received for publication 27 February 2006 and accepted in revised form 16 June 2006.

Additional information for this article can be found in an online appendix at <http://diabetes.diabetesjournals.org>.

$[\text{Ca}^{2+}]_i$ , intracellular  $\text{Ca}^{2+}$  concentration.

DOI: 10.2337/db06-0272

© 2006 by the American Diabetes Association.

The costs of publication of this article were defrayed in part by the payment of page charges. This article must therefore be hereby marked "advertisement" in accordance with 18 U.S.C. Section 1734 solely to indicate this fact.

the level needed for insulin to be released, the frequency of  $[Ca^{2+}]_i$  oscillations diminishes, and, as a result, glucagon release decreases (12,23). The mechanism used by high glucose to abolish  $[Ca^{2+}]_i$  oscillations and glucagon release is still controversial, involving direct actions on  $\alpha$ -cells (14,17,24–26) as well as paracrine effects, mainly insulin released from neighboring  $\beta$ -cells (27–32).

The studies mentioned above have provided important data about the regulation of  $\alpha$ - and  $\beta$ -cells in the intact islets of rodents. However, there is very limited information about these cell types in humans. In the current work, we have analyzed the characteristic  $Ca^{2+}$  signaling patterns of immunoidentified  $\alpha$ - and  $\beta$ -cells within human islets, using confocal microscopy. Insulin-containing  $\beta$ -cells presented glucose-induced synchronic  $[Ca^{2+}]_i$  oscillations in clusters, although the degree of synchrony was not as widespread as in the mouse. On the contrary, glucagon-containing  $\alpha$ -cells presented an asynchronous  $[Ca^{2+}]_i$  oscillatory pattern in response to low glucose concentrations.

## RESEARCH DESIGN AND METHODS

Pancreatic glands were excised from five cadaveric organ donors at the transplantation coordination unit of the Hospital General Universitario of Alicante, Alicante, Spain. The age (means  $\pm$  SE) of the donors was  $22.6 \pm 5.3$  years. According to our institutional guidelines, a small portion from each pancreas was excised and transported in cold University of Wisconsin solution (33) to the human islets unit of our institution. Then, the fibrotic and adipose parts of the sample were removed. The tissue was minced into small pieces of 1–2 mm and digested with collagenase for 15 min at  $37^\circ C$  with manual gentle shaking (34–36). The digestion solution contained (in mmol/l): 115 NaCl, 10  $NaHCO_3$ , 5 KCl, 1.1  $MgCl_2$ , 1.2  $NaH_2PO_4$ , 2.5  $CaCl_2$ , 25 HEPES, and 5 D-glucose, pH 7.4, as well as 1% BSA and 1.4 mg/ml of the enzyme preparation Liberase (Roche, Barcelona, Spain) (37). Isolated islets were picked with a pipette under inspection in a dissection microscope and then placed in a cell culture chamber at  $37^\circ C$  for 30 min before loading with  $Ca^{2+}$  probes. After this period, single islets were loaded with 5  $\mu mol/l$  of the  $Ca^{2+}$  probe Fluo-3 (acetoxymethyl derivative; Molecular Probes, Madrid, Spain) for at least 1 h at room temperature, as previously reported (12,13), in a medium containing (in mmol/l): 115 NaCl, 10  $NaHCO_3$ , 5 KCl, 1.1  $MgCl_2$ , 1.2  $NaH_2PO_4$ , 2.5  $CaCl_2$ , and 25 HEPES, as well as 1% BSA and 5 mmol/l D-glucose, pH 7.4. All experiments were carried out at  $37^\circ C$ .

**Confocal imaging microscopy of cytosolic  $Ca^{2+}$ .** For imaging experiments, islets were placed in a perfusion chamber mounted on the stage of the microscope and allowed to attach onto poly-L-lysine-treated coverslips for 10 min before starting experiments. Islets were then perfused at a rate of 1.5 ml/min with a modified Ringer solution containing (in mmol/l): 120 NaCl, 5 KCl, 25  $NaHCO_3$ , 1.1  $MgCl_2$ , and 2.5  $CaCl_2$ , pH 7.35, when gassed with 95%  $O_2$  and 5%  $CO_2$ .  $Ca^{2+}$  measurements were performed in individual cells with a Zeiss LSM 510 laser confocal microscope equipped with a  $40\times$  oil immersion objective (numerical aperture = 1.3). The system configuration was set to excite the  $Ca^{2+}$  probe at 488 nm and collect the emission with a bandpass filter at 505–530 nm from an optical section of 8  $\mu m$ . Images were collected at 2- to 4-s intervals. Temporal series were treated with a low-pass filter and processed, using the digital image software of the Zeiss LSM 510 confocal microscope (12,13,38).

Individual cells loaded with the fluorescent  $Ca^{2+}$  reporter were easily identified at the periphery of the islet (Fig. 1). It has been previously reported in the islet and other specimens that fluorescent probes have difficulty penetrating the center of thick samples (12,39). However, this is not a problem because all of the cell types are present in the peripheral layers of the islet (5,12).

**Immunocytochemistry.** After  $Ca^{2+}$  signals were recorded in an optical section, intact islets were washed with PBS for 10 min, fixed using 4% (wt/vol) paraformaldehyde for 10 min, and permeabilized with 0.5% Triton X-100 for 10 min, as previously described (12,13,40). To reduce nonspecific antibody binding, cells were first preincubated with a blocking buffer (2% goat serum in PBS) for 15 min at room temperature before primary antibodies were applied in the same buffer. An anti-insulin monoclonal antibody (5.2 mg/ml, 1:1,000 dilution; Sigma, Barcelona, Spain) or an anti-glucagon monoclonal antibody (17 mg/ml, 1:1,000 dilution; Sigma) were applied for 2 h. After washing, fluorescein isothiocyanate-conjugated secondary antibodies were applied for 1 h to visualize staining; a goat anti-mouse antibody (1.1 mg/ml, 1:64 dilution;

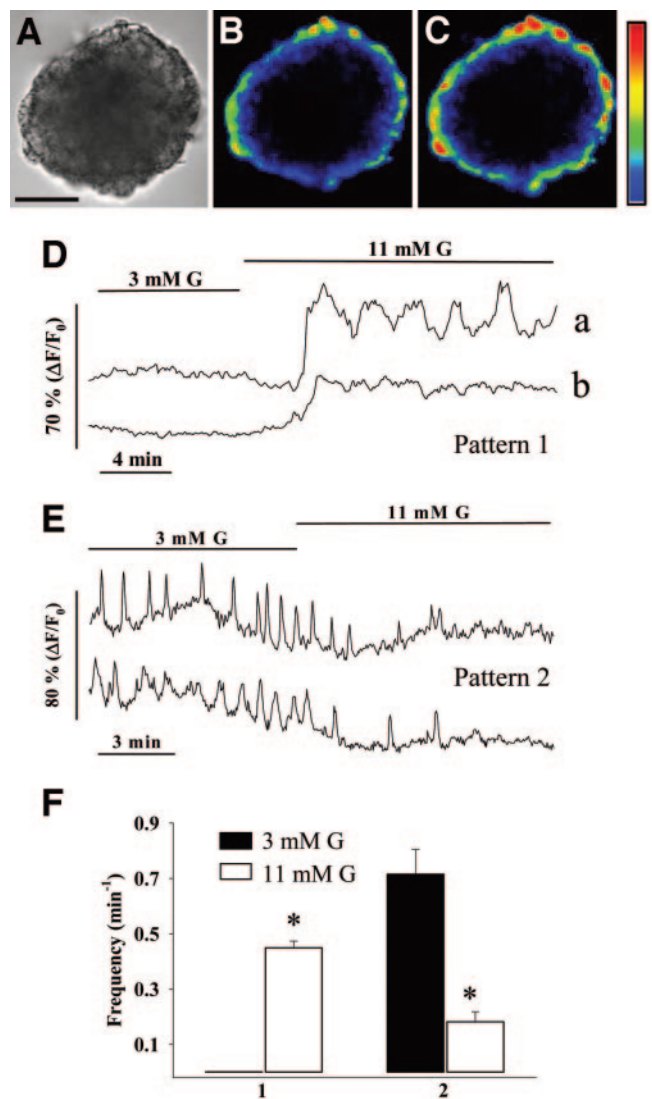


**FIG. 1.** Fluorescence changes monitored from individual cells within intact human islets of Langerhans. **A:** Transmission image of an intact human islet of Langerhans. **B:** Color image of the same islet of Langerhans as in panel **A** loaded with the  $Ca^{2+}$ -sensitive dye Fluo-3 and exposed to 3 mmol/l glucose (G). **C:** Color image of the same islet of Langerhans as in panel **A** loaded with the  $Ca^{2+}$ -sensitive dye Fluo-3 and exposed to 11 mmol/l glucose. Fluorescence images were acquired from an 8- $\mu m$  optical section close to the equatorial plane. Note that individual cells loaded with the fluorescent  $Ca^{2+}$  reporter were easily identified at the periphery of the islet. Bar = 60  $\mu m$  (color scale: blue, low  $[Ca^{2+}]_i$ ; red, high  $[Ca^{2+}]_i$ ). **D:** Records of fluorescence intensity versus time from an islet as shown in panel **A**. Increasing glucose concentration from 3 to 11 mmol/l produced a rise in the fluorescence of several cells. The majority of cells were silent at 3 mmol/l glucose ( $n = 41$ , pattern 1). However, a change to 11 mmol/l produced either  $[Ca^{2+}]_i$  oscillations ( $n = 35$ , pattern 1a) or a sustained increase ( $n = 6$ , pattern 1b). **E:** In some cells, a low concentration of glucose produced oscillations of  $[Ca^{2+}]_i$  ( $n = 13$ , pattern 2). These signals were abolished or their frequency markedly reduced when the glucose concentration was increased to 11 mmol/l. **F:** Oscillatory frequency of the  $Ca^{2+}$  signals at 3 and 11 mmol/l glucose for both groups of cells (patterns 1a and 2). Data are the means  $\pm$  SE ( $P < 0.01$ , Student's *t* test).  $Ca^{2+}$  signals were analyzed in 61 cells of 10 islets (see Table 1).

Sigma) was used for insulin or glucagon. Fluorescence was visualized, using the same confocal system. The same optical section was maintained during the entire protocol as previously described (12,13). For that purpose, during immunocytochemistry, the preparation was continuously monitored by acquiring images (one image per minute) in the transmitted light channel of the confocal microscope with a wavelength different from that used for immunodetection. Additionally, to avoid any movement of the sample derived from manipula-

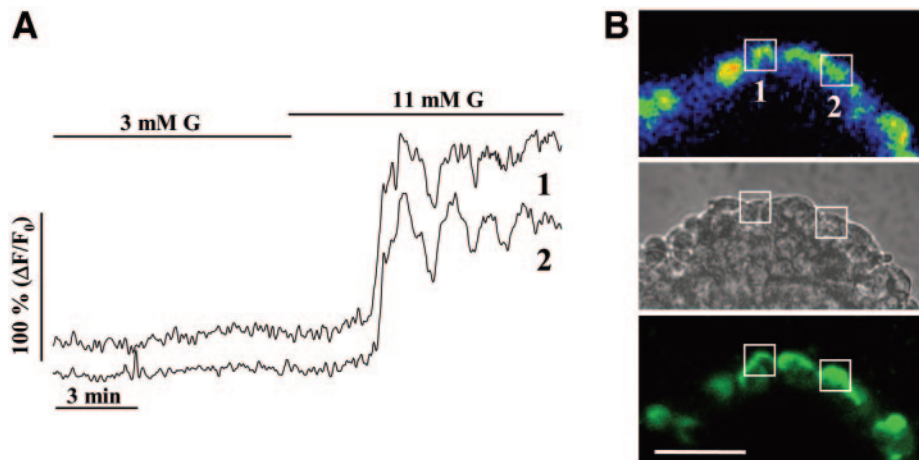


**FIG. 2.** Identification of the characteristic  $\beta$ -cell response to glucose (G). After recording  $\text{Ca}^{2+}$  signals,  $\beta$ -cells were identified in the same optical section by immunocytochemistry against insulin. **A:** Glucose-induced  $\text{Ca}^{2+}$  signaling patterns of the two cells indicated in panel **B**. Note a high level of synchronicity between both patterns. **B:** The distribution of the cells loaded with the fluorescent  $\text{Ca}^{2+}$  probe Fluo-3 (upper picture), a transmitted light image after fixation (middle picture), and the immunofluorescence of the same area and optical section of the islet (lower picture). White squares in each image indicate the position of the two cells whose  $\text{Ca}^{2+}$  signals are shown in panel **A**. This correspondence between the  $\text{Ca}^{2+}$  pattern and the immunocytochemistry is representative of 15 identifications from two samples. Scale bar = 50  $\mu\text{m}$ .

tion, we applied all of the components of the immunocytochemistry with the perfusion system at a very low rate of flux. Because of the preparation's thickness, it is difficult for antibodies to stain the center of the whole islet, as has been previously reported (12–14). However, this is not a limitation for our experiments because the areas surrounding the center include all of the cell types that form the islet (5,12). Other protocols that allow the staining of deeper cell layers in the islet involve multiple steps and overnight incubations. These protocols, however, are impractical in our experimental design because the islet has to be kept in the same position under the microscope to correlate  $\text{Ca}^{2+}$  records with the cell staining in the same optical section. Identification of islet cells, by immunocytochemistry after  $\text{Ca}^{2+}$  signal recordings, was performed in only a fraction of the experiments, as indicated in Figs. 2 and 3. **Insulin secretion.** Human islets were cultured for 24 h in Miami culture medium. Then, groups of five islets per chamber were washed with fresh Krebs-Ringer buffer and incubated in a 5%  $\text{CO}_2/95\%$   $\text{O}_2$  tissue culture cabinet for 1 h at 37°C in 0.5 ml Krebs-Ringer buffer with 0.5% BSA and 3 mmol/l glucose. This medium was then replaced with fresh buffer, and the islets were exposed for 1 h to 0.5 ml of the same buffer with 3, 8.3, or 22 mmol/l glucose. Later, the culture supernatants were collected. To measure the insulin content, islets were washed with PBS and extracted with 0.18 N HCl in 70% ethanol for 24 h at 4°C. The acid-ethanol eluates were collected. Insulin was assayed by radioimmunoassay, using human insulin as standard. The purpose of these secretion assays was only to check that the human islets used in these experiments had a normal secretory response to glucose (41).

**Statistical analysis and data representation.** Fluorescence records were represented as the percentage of  $\Delta F/F_0$ , where  $F_0$  is the fluorescence signal at the beginning of a record and  $\Delta F = F - F_0$ . Background fluorescence was subtracted from  $F_0$ . Student's *t* test was performed with commercial software (SigmaPlot; Jandel, San Rafael, CA). Some data are shown as the means  $\pm$  SE.

## RESULTS

**Measuring  $[\text{Ca}^{2+}]_i$  in individual cells within intact human islets.** To investigate the effect of glucose on individual  $\alpha$ - and  $\beta$ -cells,  $[\text{Ca}^{2+}]_i$  recordings were obtained from intact human islets of Langerhans (Fig. 1A) loaded with the  $\text{Ca}^{2+}$ -sensitive fluorescent dye Fluo-3 and imaged using laser scanning confocal microscopy (Fig. 1B and C). Although only the periphery of the islet was loaded, as previously described (12,13,42), all of the different cell types are represented in the outer cell layers of the human islet (5,6). Islets obtained for these experiments presented normal insulin content ( $44 \pm 14$  ng insulin/ $\mu\text{g}$  protein, four different experiments) and a regular response to glucose in terms of insulin release (online appendix Fig. 1 [available at <http://diabetes.diabetesjournals.org>]), indicating their viability and normal function.

Different  $[\text{Ca}^{2+}]_i$  signaling patterns were recorded in individual cells within islets depending on the extracellular glucose concentration. Figure 1D shows two representative traces in which  $[\text{Ca}^{2+}]_i$  remains constant at low glucose concentrations (3 mmol/l), yet when an extracellular glucose concentration of 11 mmol/l was perfused, an increase in  $[\text{Ca}^{2+}]_i$  was observed. This rise in  $[\text{Ca}^{2+}]_i$  was followed by either  $[\text{Ca}^{2+}]_i$  oscillations on a plateau (in 35 cells of 61 from 10 islets) (Fig. 1D, pattern 1a, and Table 1) or a plateau without  $[\text{Ca}^{2+}]_i$  oscillations (6 of 61 cells from 10 islets) (Fig. 1D, pattern 1b). The frequency of  $\text{Ca}^{2+}$  oscillations is represented in Fig. 1F and Table 1. These  $\text{Ca}^{2+}$  patterns resemble those previously described for  $\beta$ -cells in both humans (34,36,43) and mice (12,20–22,44) (see below).

The second typical pattern was opposite to that described above. In this case, some cells presented an oscillatory  $[\text{Ca}^{2+}]_i$  signal at a low glucose concentration (3 mmol/l), and the frequency of these oscillations was highly diminished in the presence of an insulin-stimulating glucose concentration (11 mmol/l, 13 of 61 cells from 10 islets) (Fig. 1E and F and Table 1, pattern 2). This pattern is identical to that described in mice for glucagon-containing  $\alpha$ -cells (12,13) (see below).

To unequivocally identify the different types of glucose-modulated  $\text{Ca}^{2+}$  signals, cells were stained by immunocytochemistry after monitoring their glucose-induced  $[\text{Ca}^{2+}]_i$  pattern. Cells displaying a  $[\text{Ca}^{2+}]_i$  signal similar to that shown in Figs. 1D and 2A were identified as insulin-containing  $\beta$ -cells (Fig. 2B). On the other hand, those cells presenting a  $[\text{Ca}^{2+}]_i$  pattern opposite to that observed in the  $\beta$ -cell, as shown in Figs. 1E and 3A, were identified as glucagon-containing  $\alpha$ -cells (Fig. 3B). Note that cells with a  $\beta$ -cell  $[\text{Ca}^{2+}]_i$  response were not stained with anti-glucagon antibodies. Human pancreatic  $\alpha$ -cells respond to glucose in a dose-dependent manner: the lower the extracellular glucose concentration, the higher the frequency of  $[\text{Ca}^{2+}]_i$  oscillations (Fig. 3C). Additionally, a few cells presented an oscillatory pattern at 3 mmol/l glucose that was not inhibited by high glucose concentration (7 of 61 cells) (Fig. 6 and Table 1, pattern 3).

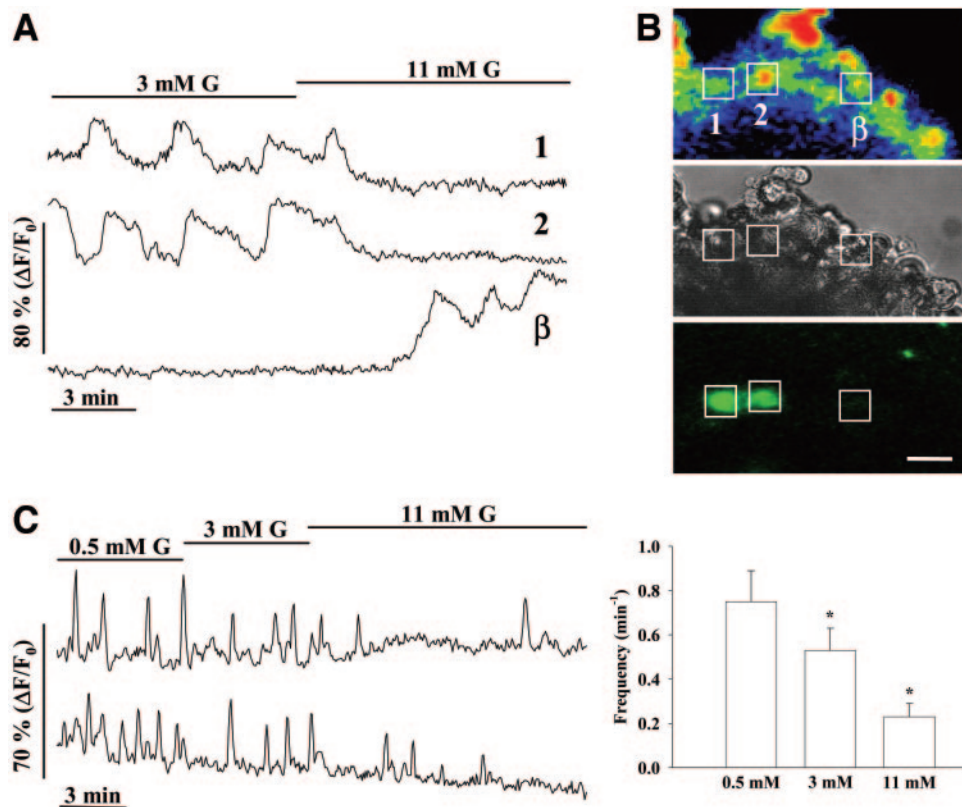


**FIG. 3.** Identification of the characteristic  $\alpha$ -cell response to glucose (G). We proceeded with the same protocol used in Fig. 2. Subsequent to recording  $\text{Ca}^{2+}$  signals,  $\alpha$ -cells were identified in the same optical section by immunocytochemistry, using anti-glucagon antibodies. **A:** Glucose-induced  $\text{Ca}^{2+}$  signaling patterns of the two  $\alpha$ -cells indicated in *panel B* together with the response of a  $\beta$ -cell. Note that both signaling patterns are opposite. **B:** The distribution of the cells loaded with the fluorescent  $\text{Ca}^{2+}$  probe Fluo-3 (*upper picture*), a transmitted light image after fixation (*middle panel*), and the immunofluorescence of the same area and optical section of the islet (*lower picture*). White squares in each image indicate the position of the three cells whose  $\text{Ca}^{2+}$  signals are shown in *panel A*. This correspondence between the  $\text{Ca}^{2+}$  pattern and the immunocytochemistry is representative of five identifications from three samples. Scale bar = 50  $\mu\text{m}$ . **C:**  $\text{Ca}^{2+}$  records illustrate the effect on  $\alpha$ -cells of 0.5, 3, and 11 mmol/l glucose. The horizontal lines above the traces indicate the periods of application of the different glucose concentrations. The graph on the right shows the glucose-induced changes in frequency of the  $\text{Ca}^{2+}$  signals ( $n = 5$ ). \* $P < 0.05$ , Student's  $t$  test comparing both columns with 0.5 mmol/l glucose.

**Synchronicity of the  $[\text{Ca}^{2+}]_i$  response.** The behavior of the human islet as a syncytium in terms of  $[\text{Ca}^{2+}]_i$  signaling is still controversial. Although some studies suggested that human islets function as a syncytium (34,36,43), others have reported an opposite view (6). The experiment shown in Fig. 4A demonstrates that  $\beta$ -cells within human islets work in synchrony in clusters (Fig. 4A, *photograph inset*), although  $\text{Ca}^{2+}$  signals between different clusters are asynchronous (four of seven islets analyzed). In a few cases, uncoordinated groups of cells exhibited a synchronic response after several minutes of glucose stimulation. For instance, Fig. 4B illustrates four traces from different cells of two clusters within the same islet (Fig. 4B, *photograph inset*). In this experiment, some cells have a

uncoordinated initial response that synchronizes several minutes later ( $\sim 6$  min). This particular case might indicate the involvement of paracrine factors released from glucose-stimulated cells that could increase the level of coupling between some cells. In those islets with synchronic behavior in clusters, we also observed some uncoordinated cells. The degree of synchrony varied between islets, even from the same preparation. Actually, some islets (three of seven) presented a low level of coupling between individual cells, as shown in Fig. 4C. Because we used confocal microscopy, we only measured  $\text{Ca}^{2+}$  signals from an optical slice. For that reason, synchrony between cells of the same cluster may have existed in these islets with a lower level of

**TABLE 1**  
Summary of the different calcium signaling patterns induced by glucose

Pattern	Response to glucose		Cells	Percentage	Frequency ( $\text{min}^{-1}$ )	
	3 mmol/l	11 mmol/l			3 mmol/l	11 mmol/l
1	(-)	(+)	35 (oscillations)/6 (sustained increase)	57.37/9.83	0	$0.45 \pm 0.02^*$
2	(+)	(-)	13	21.3	$0.71 \pm 0.09$	$0.18 \pm 0.03^*$
3	(+)	(+)	7	11.4	$0.91 \pm 0.24$	$0.93 \pm 0.19$ (NS)
Total	—	—	61 (10 islets)	100	—	—

Frequency data are means  $\pm$  SE. The frequency of only six cells was analyzed in pattern 3 (see Fig. 6). \* $P < 0.01$ . NS, nonsignificant.

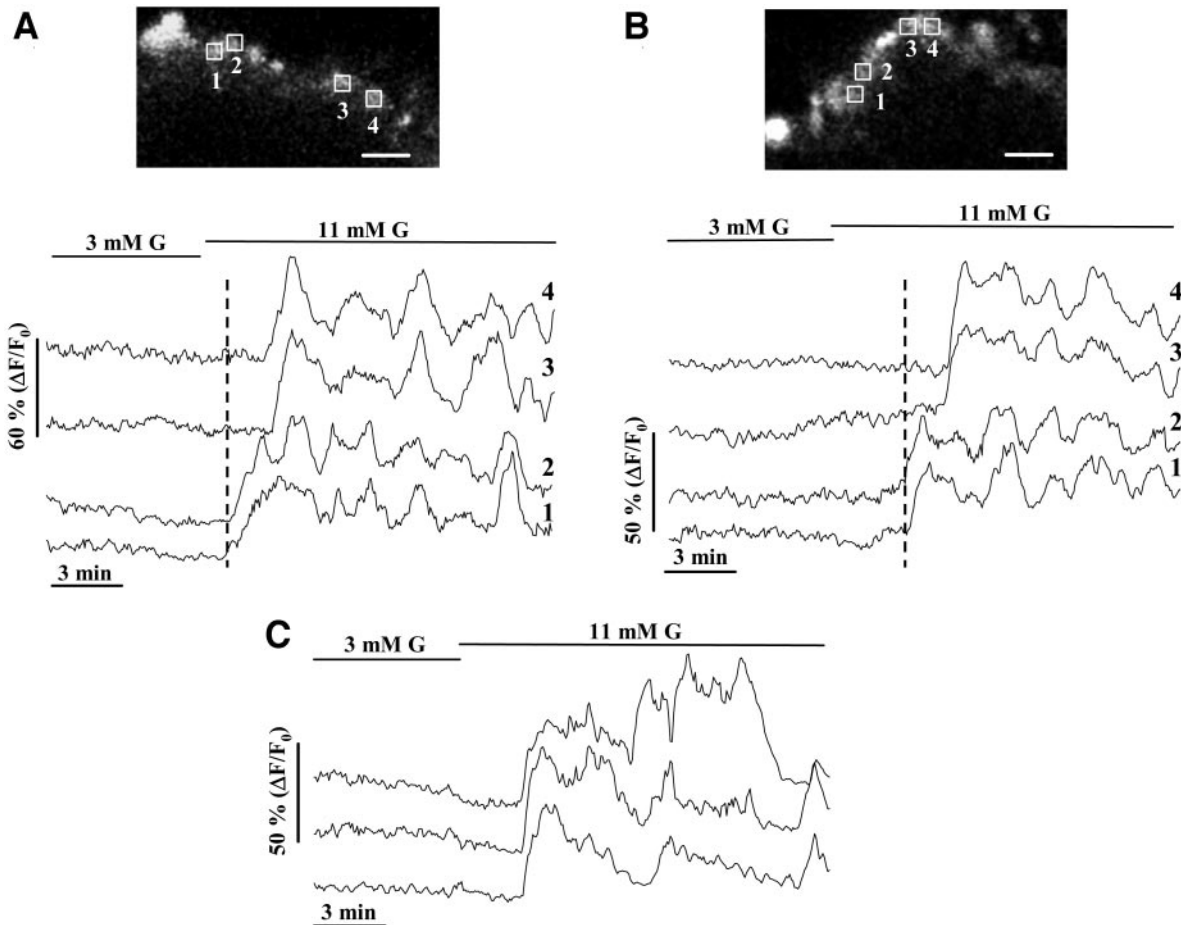


FIG. 4. Synchronicity of the response in the  $\beta$ -cell population. The glucose (G)-induced  $\text{Ca}^{2+}$  signals of several individual cells within the same islet are illustrated in each figure. Although a high degree of synchronicity was monitored among cells of the same cluster, there was a low level of coordination among different groups. A cell cluster within the islet was considered when more than two  $\beta$ -cells in physical contact presented a synchronous response in  $\text{Ca}^{2+}$  oscillations. **A:** The recordings of two groups of cells are shown. The responses of cells 1 and 2 are synchronized and start earlier than the synchronized signals of cells 3 and 4. Note that there is no coordination between both groups (cells 1 and 2 and cells 3 and 4), which show several out-of-phase oscillations. The dotted line indicates the beginning of the earlier response. The position of these cells in the islet is shown in the *upper panel*, which displays the Fluo-3 fluorescence distribution. **B:** The  $\text{Ca}^{2+}$  signal of two groups of cells is also shown. Note that there is a delay in the glucose-induced  $\text{Ca}^{2+}$  response of cells 3 and 4 compared with cells 1 and 2, although several minutes later a synchronization of their  $\text{Ca}^{2+}$  signals is observed. The position of these cells in the islet is shown in the *upper panel*, which displays the Fluo-3 fluorescence distribution. **C:** In some islets, there was either a low level of synchronicity, or cells were completely unsynchronized.

coordination in planes above and beneath the one we were measuring from. In the case of the  $\alpha$ -cell population, a high degree of asynchrony was found among cells of the same islet at any glucose concentration tested (Fig. 5). Asynchrony was also manifested among a

population of cells with an  $[\text{Ca}^{2+}]_i$  pattern identical to that of  $\delta$ -cells in mice (Fig. 6 and Table 1, *pattern 3*) (12,13). Nonetheless, because of the scarcity of cells with this  $[\text{Ca}^{2+}]_i$  pattern, it was impractical to unequivocally identify them by immunocytochemistry.

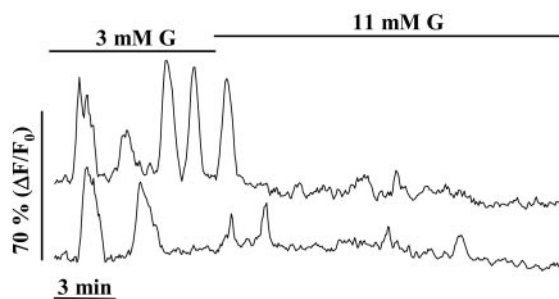


FIG. 5. Asynchrony among  $\alpha$ -cells. The  $\text{Ca}^{2+}$  signals of a couple of individual  $\alpha$ -cells within the same islet are illustrated, indicating the existence of a high level of asynchrony in this cell population. This experiment is representative of five couples of  $\alpha$ -cells analyzed in different islets. Figures 3A and C show more examples of pairs of asynchronous  $\alpha$ -cells within the same islet. G, glucose.

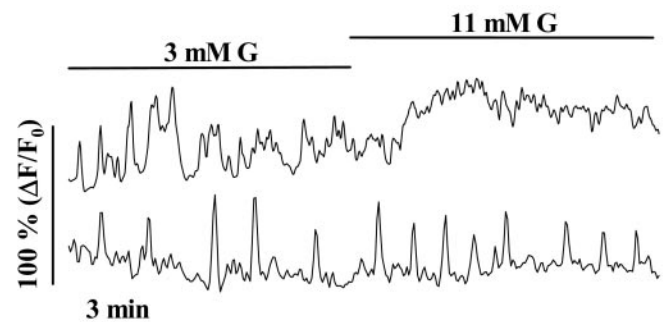


FIG. 6. Of the cells, 10% (6 of 61 cells from 10 islets) produced oscillatory  $\text{Ca}^{2+}$  signals at low and high glucose concentrations without significant changes in frequency (*lower trace*) (also see Table 1). Only one cell oscillating in 3 mmol/l responded with a small sustained increase when glucose was elevated to 11 mmol/l (*upper trace*).

## DISCUSSION

The work presented here shows the glucose-induced  $[Ca^{2+}]_i$  patterns of identified  $\alpha$ - and  $\beta$ -cells within intact human islets of Langerhans. Changes in  $[Ca^{2+}]_i$  play a fundamental role in insulin concentration and glucagon secretion (12,13,25,45–47). High glucose generated  $[Ca^{2+}]_i$  oscillations with a frequency of  $0.45 \pm 0.02 \text{ min}^{-1}$  in individual human  $\beta$ -cells within the islet that represented a proper insulin release in response to glucose. In the majority of cases, the amplitude of the oscillations monitored with the probe Fluo-3 was slightly smaller than previous recordings obtained in mice (12), although a ratiometric probe would be more reliable for measuring the amplitude of these oscillations. In any case, the  $Ca^{2+}$  signals described in the current work were similar to those reported previously in whole human islets (34,36,43). Nonetheless, the use of confocal microscopy has allowed us to deeply study the individual  $[Ca^{2+}]_i$  signals in single cells within intact islets and also to compare cell-to-cell characteristics. We have found that the degree of synchrony of  $[Ca^{2+}]_i$  oscillations among individual  $\beta$ -cells was lower than in mice, displaying a more heterogeneous response. First,  $\beta$ -cells within the same human islet presented different types of responses, as shown in Figs. 1D and 4, rather than the same  $[Ca^{2+}]_i$  pattern in all of the  $\beta$ -cells within the islet, as has been reported in mice (12). Second, a synchronicity in the oscillatory pattern was visualized in different  $\beta$ -cells in groups, although this response lacked coordination among clusters within the same islet. Moreover, a moderated asynchrony was manifested during the initiation of the glucose-induced  $[Ca^{2+}]_i$  response in some grouped  $\beta$ -cells within the same islet (see Fig. 4B).

This kind of pattern, including a synchronic oscillatory  $[Ca^{2+}]_i$  response between  $\beta$ -cells in groups and also uncoordinated signals from individual cells, should be a consequence of the human islet architecture (4–6). The human islet contains a larger number of  $\alpha$ -cells than other species and a clustered distribution of the  $\beta$ -cell population (4–6) instead of a continuous cell mass which, in the case of mice, leads to a functional syncytium (7,12,20). In this animal model, it is well known that junctional communication and a synchronic function of the whole  $\beta$ -cell population is essential for appropriate control of both  $[Ca^{2+}]_i$  signals and insulin release (48–50). In humans, the situation is different:  $\beta$ -cell clusters tend to work as coordinated units in terms of  $[Ca^{2+}]_i$  signals, yet glucose-induced  $[Ca^{2+}]_i$  patterns are different between clusters within the same islet. Nonetheless, new studies are necessary to determine how the cluster organization of human  $\beta$ -cells affects the oscillatory behavior of insulin secretion (51–54).

A second group of cells presented an opposite  $[Ca^{2+}]_i$  pattern in response to glucose. Low glucose concentrations generated nonsynchronic  $[Ca^{2+}]_i$  oscillations, a signal that was rendered silent in the presence of a high extracellular glucose concentration (11 mmol/l). This cell group was identified as glucagon-containing  $\alpha$ -cells by immunocytochemistry. The frequency of these  $[Ca^{2+}]_i$  oscillations in  $\alpha$ -cells was  $0.71 \pm 0.09 \text{ min}^{-1}$ , which is well within the range of  $\alpha$ -cells from mouse islets ( $0.81 \pm 0.09 \text{ min}^{-1}$ ) (12,13). The low-glucose-induced  $[Ca^{2+}]_i$  oscillations in  $\alpha$ -cells were nonsynchronic, as is the case in mouse islets (12). This is consistent with the idea that these cells function individually within the islet to secrete

glucagon rather than act as a syncytium. Similar to the situation in mice,  $\alpha$ -cells are spatially distributed as single units or in small groups in the human islet (4–6).

In addition to a direct effect of glucose, insulin and glucagon as well as other paracrine signals are important modulators of  $\beta$ - and  $\alpha$ -cell function in several species (27–32). Given the absence of exhaustive studies in human islet cell physiology, further analysis of these other regulators is required to have a more complete view of the functional organization of these cell populations. The current study describes  $Ca^{2+}$  signaling patterns in response to glucose of  $\alpha$ - and  $\beta$ -cells within the human intact islet, a preparation whose behavior is closer to the physiological scenario (12,13,21,22). Because several structural and functional differences between animal models and humans have been reported (4–6,36), the information presented here is important to understand the physiology of these cell types in the human endocrine pancreas and the regulation of glucose homeostasis. In addition, these data provide a criterion to identify these cell types within the islet in other functional studies. A better understanding of the physiology of the human islet can also provide criteria to evaluate its optimal function, which may help to improve the selection of high-quality islets for transplantation (3).

## ACKNOWLEDGMENTS

This work was supported in part by Ministerio de Ciencia y Tecnología Grant SAF2004-07483-C04-01; Instituto de Salud Carlos III Grants GO3/171, GO3/210, and GO3/212 (to B.S.) and Red de Centros de Metabolismo y Nutrición 03/08 (to A.N.); Ministerio de Educación y Ciencia Grants BFU2004-07283 (to I.Q.) and BFU2005-01052 (to A.N.); and Conselho Nacional de Desenvolvimento Científico e Tecnológico Brazil Grant 200001/03-5 (to E.M.C.).

The authors thank Begoña Fernandez and Mónica Navarro Barreto for expert technical assistance and C. Santiago, P. Gómez, and L. Pérez from the Transplantation Coordination Unit of the Hospital General Universitario de Alicante.

## REFERENCES

- Shapiro AMJ, Lakey JRT, Ryan EA, Korbitt GS, Toth EL, Warnock GL, Kneteman NN, Rajotte RV: Islet transplantation in seven patients with type 1 diabetes mellitus using a glucocorticoid-free immunosuppressive regimen. *N Engl J Med* 343:230–238, 2000
- Nanji SA, Shapiro AM: Advances in pancreatic islet transplantation in humans. *Diabetes Obes Metab* 8:15–25, 2006
- Ichii H, Inverardi L, Pileggi A, Molano RD, Cabrera O, Caicedo A, Messinger S, Kuroda Y, Berggren PO, Ricordi C: A novel method for the assessment of cellular composition and beta-cell viability in human islet preparations. *Am J Transplant* 5:1635–1645, 2005
- Orci L, Unger RH: Functional subdivision of islets of Langerhans and possible role of D cells. *Lancet* 2:1243–1244, 1975
- Brissova M, Fowler MJ, Nicholson WE, Chu A, Hirshberg B, Harlan DM, Powers AC: Assessment of human pancreatic islet architecture and composition by laser scanning confocal microscopy. *J Histochem Cytochem* 53:1087–1097, 2005
- Cabrera O, Berman DM, Kenyon NS, Ricordi C, Berggren PO, Caicedo A: The unique cytoarchitecture of human pancreatic islets has implications for islet cell function. *Proc Natl Acad Sci U S A* 103:2334–2339, 2006
- Kanno T, Gopel SO, Rorsman P, Wakui M: Cellular function in multicellular system for hormone-secretion: electrophysiological aspect of studies on alpha-, beta- and delta-cells of the pancreatic islet. *Neurosci Res* 42:79–90, 2002
- Prentki M, Matchinsky FM:  $Ca^{2+}$ , cAMP and phospholipid-derived messengers in coupling mechanisms of insulin secretion. *Physiol Rev* 67:1185–1248, 1987

9. Unger RH: Glucagon and insulin: a bihormonal system. *Compr Ther* 2:20–26, 1976
10. Soria B, Andreu E, Berna G, Fuentes E, Gil A, Leon-Quinto T, Martin F, Montanya E, Nadal A, Reig JA, Ripoll C, Roche E, Sanchez-Andres JV, Segura J: Engineering pancreatic islets. *Pflugers Arch* 440:1–18, 2000
11. Berts A, Gylfe E, Hellman B:  $Ca^{2+}$  oscillations in pancreatic islet cells secreting glucagon and somatostatin. *Biochem Biophys Res Commun* 208:644–649, 1995
12. Nadal A, Quesada I, Soria B: Homologous and heterologous asynchronicity between identified alpha-, beta- and delta-cells within intact islets of Langerhans in the mouse. *J Physiol* 517:85–93, 1999
13. Quesada I, Nadal A, Soria B: Different effects of tolbutamide and diazoxide in  $\alpha$ -,  $\beta$ -, and  $\delta$ -cells within intact islets of Langerhans. *Diabetes* 48:2390–2397, 1999
14. Gopel SO, Kanno T, Barg S, Weng XG, Gromada J, Rorsman P: Regulation of glucagon release in mouse alpha-cells by  $K_{ATP}$  channels and inactivation of TTX-sensitive  $Na^+$  channels. *J Physiol* 528:509–520, 2000
15. Barg S, Galvanovskis J, Gopel SO, Rorsman P, Eliasson L: Tight coupling between electrical activity and exocytosis in mouse glucagon-secreting  $\alpha$ -cells. *Diabetes* 49:1500–1510, 2000
16. Martin F, Andreu E, Rovira JM, Pertusa JA, Raurell M, Ripoll C, Sanchez-Andres JV, Montanya E, Soria B: Mechanisms of glucose hypersensitivity in  $\beta$ -cells from normoglycemic, partially pancreatectomized mice. *Diabetes* 48:1954–1961, 1999
17. Unger RH: Glucagon physiology and pathophysiology in the light of new advances. *Diabetologia* 28:574–578, 1985
18. Dinneen S, Alzaid A, Turk D, Rizza R: Failure of glucagon suppression contributes to postprandial hyperglycaemia in IDDM. *Diabetologia* 38:337–343, 1995
19. Gerich JE: Lilly lecture 1988. Glucose counterregulation and its impact on diabetes mellitus. *Diabetes* 37:1608–1617, 1988
20. Santos RM, Rosario LM, Nadal A, Garcia-Sancho J, Soria B, Valdeolmillos M: Widespread synchronous  $[Ca^{2+}]_i$  oscillations due to bursting electrical activity in single pancreatic islets. *Pflugers Arch* 418:417–422, 1991
21. Sanchez-Andres JV, Gomis A, Valdeolmillos M: The electrical activity of mouse pancreatic beta-cells recorded in vivo shows glucose-dependent oscillations. *J Physiol* 486:223–228, 1995
22. Fernandez J, Valdeolmillos M: Synchronous glucose-dependent  $[Ca^{2+}]_i$  oscillations in mouse pancreatic islets of Langerhans recorded in vivo. *FEBS Lett* 477:33–36, 2000
23. Opara EC, Atwater I, Go VL: Characterization and control of pulsatile secretion of insulin and glucagon. *Pancreas* 3:484–487, 1988
24. Liu YJ, Vieira E, Gylfe E: A store-operated mechanism determines the activity of the electrically excitable glucagon-secreting pancreatic alpha-cell. *Cell Calcium* 35:357–365, 2004
25. Gromada J, Ma X, Hoy M, Bokvist K, Salehi A, Berggren PO, Rorsman P: ATP-sensitive  $K^+$  channel-dependent regulation of glucagon release and electrical activity by glucose in wild-type and SUR1-/- mouse  $\alpha$ -cells. *Diabetes* 53 (Suppl. 3):S181–S189, 2004
26. Olsen HL, Theander S, Bokvist K, Buschard K, Wollheim CB, Gromada J: Glucose stimulates glucagon release in single rat alpha-cells by mechanisms that mirror the stimulus-secretion coupling in beta-cells. *Endocrinology* 146:4861–4870, 2005
27. Ravier MA, Rutter GA: Glucose or insulin, but not zinc ions, inhibit glucagon secretion from mouse pancreatic  $\alpha$ -cells. *Diabetes* 54:1789–1797, 2005
28. Ostenson CG: Regulation of glucagon release: effects of insulin on the pancreatic A2-cell of the guinea pig. *Diabetologia* 17:325–330, 1979
29. Ishihara H, Maechler P, Gjinovci A, Herrera PL, Wollheim CB: Islet beta-cell secretion determines glucagon release from neighbouring alpha-cells. *Nat Cell Biol* 5:330–335, 2003
30. Wendt A, Birnir B, Buschard K, Gromada J, Salehi A, Sewing S, Rorsman P, Braun M: Glucose inhibition of glucagon secretion from rat  $\alpha$ -cells is mediated by GABA released from neighboring  $\beta$ -cells. *Diabetes* 53:1038–1045, 2004
31. Leung YM, Ahmed I, Sheu L, Gao X, Hara M, Tsumishima RG, Diamant NE, Gaisano HY: Insulin regulates islet alpha-cell function by reducing  $K_{ATP}$  channel sensitivity to ATP inhibition. *Endocrinology* 147:2155–2162, 2006
32. Franklin I, Gromada J, Gjinovci A, Theander S, Wollheim CB:  $\beta$ -Cell secretory products activate  $\alpha$ -cell ATP-dependent potassium channels to inhibit glucagon release. *Diabetes* 54:1808–1815, 2005
33. Kinasiewicz A, Juszcak M, Pachecka J, Fiedor P: Pancreatic islets isolation using different protocols with in situ flushing and intraductal collagenase injection. *Physiol Res* 53:327–333, 2004
34. Kindmark H, Kohler M, Nilsson T, Arkhammar P, Wiechel KL, Rorsman P, Efendic S, Berggren PO: Measurements of cytoplasmic free  $Ca^{2+}$  concentration in human pancreatic islets and insulinoma cells. *FEBS Lett* 291:310–314, 1991
35. Kindmark H, Kohler M, Arkhammar P, Efendic S, Larsson O, Linder S, Nilsson T, Berggren PO: Oscillations in cytoplasmic free  $Ca^{2+}$  concentration in human pancreatic islets from subjects with normal and impaired glucose tolerance. *Diabetologia* 37:1121–1131, 1994
36. Hellman B, Gylfe E, Bergsten P, Grapengiesser E, Lund PE, Berts A, Tengholm A, Pipeleers DG, Ling Z: Glucose induces oscillatory  $Ca^{2+}$  signalling and insulin release in human pancreatic beta cells. *Diabetologia* 37 (Suppl. 2):S11–S20, 1994
37. Bucher P, Mathe Z, Bosco D, Andres A, Kurfuerst M, Ramsch-Gunther N, Buhler L, Morel P, Berney T: Serva collagenase NB1: a new enzyme preparation for human islet isolation. *Transplant Proc* 36:1143–1144, 2004
38. Quesada I, Rovira JM, Martin F, Roche E, Nadal A, Soria B: Nuclear  $K_{ATP}$  channels trigger nuclear  $Ca^{2+}$  transients that modulate nuclear function. *Proc Natl Acad Sci U S A* 99:9544–9549, 2002
39. Nadal A, Sul JY, Valdeolmillos M, McNaughton PA: Albumin elicits calcium signals from astrocytes in brain slices from neonatal rat cortex. *J Physiol* 509:711–716, 1998
40. Asada N, Shibuya I, Iwanaga T, Niwa K, Kanno T: Identification of  $\alpha$ - and  $\beta$ -cells in intact isolated islets of Langerhans by their characteristic cytoplasmic  $Ca^{2+}$  concentration dynamics and immunocytochemical staining. *Diabetes* 47:751–757, 1998
41. Ricordi C, Gray DW, Hering BJ, Kaufman DB, Warnock GL, Kneteman NM, Lake SP, London NJ, Socci C, Alejandro R, et al.: Islet isolation assessment in man and large animals. *Acta Diabetol Lat* 27:185–195, 1990
42. Ropero AB, Soria B, Nadal A: A nonclassical estrogen membrane receptor triggers rapid differential actions in the endocrine pancreas. *Mol Endocrinol* 16:497–505, 2002
43. Martin F, Soria B: Glucose-induced  $[Ca^{2+}]_i$  oscillations in single human pancreatic islets. *Cell Calcium* 20:409–414, 1996
44. Valdeolmillos M, Santos RM, Contreras D, Soria B, Rosario LM: Glucose-induced oscillations of intracellular  $Ca^{2+}$  concentration resembling bursting electrical activity in single mouse islets of Langerhans. *FEBS Lett* 259:19–23, 1989
45. Gilon P, Shepherd RM, Henquin JC: Oscillations of secretion driven by oscillations of cytoplasmic  $Ca^{2+}$  as evidences in single pancreatic islets. *J Biol Chem* 268:22265–22268, 1993
46. Barbosa RM, Silva AM, Tome AR, Stamford JA, Santos RM, Rosario LM: Control of pulsatile 5-HT/insulin secretion from single mouse pancreatic islets by intracellular calcium dynamics. *J Physiol* 510:135–143, 1998
47. Rojas E, Carroll PB, Ricordi C, Boschero AC, Stojilkovic SS, Atwater I: Control of cytosolic free calcium in cultured human pancreatic beta-cells occurs by external calcium-dependent and independent mechanisms. *Endocrinology* 134:1771–1781, 1994
48. Andreu E, Soria B, Sanchez-Andres JV: Oscillation of gap junction electrical coupling in the mouse pancreatic islets of Langerhans. *J Physiol* 498:753–761, 1997
49. Vozzi C, Ullrich S, Charollais A, Philippe J, Orci L, Meda P: Adequate connexin-mediated coupling is required for proper insulin production. *J Cell Biol* 131:1561–1572, 1995
50. Charollais A, Gjinovci A, Huarte J, Bauquis J, Nadal A, Martin F, Andreu E, Sanchez-Andres JV, Calabrese A, Bosco D, Soria B, Wollheim CB, Herrera PL, Meda P: Junctional communication of pancreatic beta cells contributes to the control of insulin secretion and glucose tolerance. *J Clin Invest* 106:235–243, 2000
51. Stagner JI, Samols E, Weir GC: Sustained oscillations of insulin, glucagon, and somatostatin from the isolated canine pancreas during exposure to a constant glucose concentration. *J Clin Invest* 65:939–942, 1980
52. Matthews DR, Naylor BA, Jones RG, Ward GM, Turner RC: Pulsatile insulin has greater hypoglycemic effect than continuous delivery. *Diabetes* 32:617–621, 1983
53. Lefebvre PJ, Paolisso G, Scheen AJ, Henquin JC: Pulsatility of insulin and glucagon release: physiological significance and pharmacological implications. *Diabetologia* 30:443–452, 1987
54. Ritzel RA, Veldhuis JD, Butler PC: Glucose stimulates pulsatile insulin secretion from human pancreatic islets by increasing secretory burst mass: dose-response relationships. *J Clin Endocrinol Metab* 88:742–747, 2003